Broadband dielectric study on the water-concentration dependence of the primary and secondary processes for triethyleneglycol-water mixtures

Seiichi Sudo,[1,*] Naoki Shinyashiki,[2] Yuki Arima,[2] and Shin Yagihara[2]
[1]*Departiment of Physics, Musashi Institute of Technology, Tamazutsumi, Setagaya, Tokyo 158-8557, Japan*
[2]*Department of Physics, Tokai University, Hiratsuka, Kanagawa 259-1292, Japan*
(Received 8 April 2008; published 16 July 2008)

Broadband dielectric measurements for triethyleneglycol (3EG)-water mixtures with various concentrations were performed in the frequency range of 10 μHz–10 GHz and in the temperature range of 130–298 K. For each mixture, the separation of the primary (α) and secondary processes is observed below the crossover temperature, T_C. In the case of 80–100 wt % 3EG-water mixtures, the Kohlrausch-Williams-Watts–type primary process above T_C continues to the α process below T_C, and an additional secondary process is observed in the frequency range higher than that of the α process below T_C. On the other hand, the primary process for 65 and 70 wt % 3EG-water mixtures above T_C continues to the higher-frequency secondary process below T_C, and an additional α process appears at a frequency lower than that of the secondary process. The contribution of water to relaxation processes is discussed, to clarify the molecular mechanism of the separation behavior. The characteristic separation behavior of the relaxation processes for high-water-content 3EG-water mixtures is due to the existence of excess water, which cannot move cooperatively with solute 3EG molecules below T_C.

DOI: 10.1103/PhysRevE.78.011501 PACS number(s): 64.70.pm, 77.22.Gm, 61.25.Em, 82.30.Rs

I. INTRODUCTION

When a liquid is rapidly supercooled below the melting point, its structural relaxation time increases over 13 decades with decreasing temperature. This relaxation time becomes larger than the laboratory time scale below the glass transition temperature, T_g, and the system becomes a glass. Glass-forming polymers and supercooled liquids have been intensively investigated at temperature below T_g by dielectric spectroscopies, to clearly understand the molecular dynamics related to glass transition [1,2]. According to the results for many glass formers, a primary process, i.e., the structural α process, is observed. Then, T_g has often been defined as the temperature at which the relaxation time of the α process is 100 s [3–5]. The temperature dependence of the relaxation time of the α process generally obeys the Vogel-Fulcher (VF) law [6,7], and the dielectric loss spectrum is asymmetric, as described by the Kohlrausch-Williams-Watts (KWW) [8,9] or Davidson-Cole equations [10]. The molecular dynamics of the α process is generally interpreted on the basis of the molecular motion of a cooperative region [11]. An additional relaxation process, i.e., the secondary (β) process, is observed at frequencies higher than those of the α process below the crossover temperature, T_C, even for glass-forming polymer and some small molecular liquids [1,2]. It is generally shown that the temperature dependence of the relaxation time of the β process obeys the Arrhenius law, and the loss spectrum is symmetric, as described by the Cole-Cole equation. The β process is found to be universal for glass-forming liquids and polymers; hence, it is generally believed to be characteristic of "glass transition."

Various aqueous solutions, such as molecular liquids, polymers, sugar, and biopolymers, have been investigated by dielectric spectroscopy, to clarify the relaxation phenomena in the supercooled and glassy state of the aqueous solutions [12–23]. For some aqueous solutions in water rich regions, the α and β processes are observed around T_g. The relaxation times of the α process usually follow a VF-type temperature dependence, and it was considered to be due to the cooperative rearrangement of the water and solute molecules. The β process has usually been associated with the motion of water molecules in solution. The temperature dependence of the relaxation time of the β-process is usually Arrhenius-like below T_g. In our early work, we have carried out broadband dielectric measurements for 65 wt % ethyleneglycol oligomer (EGO)- and polyethyleneglycol-water mixtures with various repeat units of a solute molecule (n_{EGO}) in the temperature range of 130–300 K and in the frequency range of 1 μHz–10 GHz [16,17]. For each mixture, only one relaxation process, called the a process [1], is observed above T_C, and the α and β processes are observed below T_C. For $n_{EGO} \leqslant 2$, the a process continues to the α process below T_C, and the additional β process is observed below T_C. In contrast, for $n_{EGO} \geqslant 3$, the a process continues to the β process below T_C, and the additional α process is observed at frequencies lower than the β process below T_C. These results indicate that the α-β separation behavior markedly changes at $n_{EGO}=3$ for 65 wt % EGO-water mixtures with various n_{EGO}, and the EGO-water mixtures with $n_{EGO} \geqslant 3$ can be considered as a suitable example of the large solute-water mixtures that exhibit glass transition.

In our previous work, 65–100 wt % triethyleneglycol (3EG)-water mixtures were investigated by broadband dielectric measurement [18]. Two relaxation processes are clearly observed below about 180 K for all materials. For 65–80 wt %, the α process is brought about by the cooperative motion of solute and water molecules. The high-frequency β process is brought about by the motion of water molecules. For 90–100 wt % 3EG-water mixtures, the low-frequency α process is brought about by the cooperative motion of solute and water molecules, and its molecular mecha-

*Corresponding author.

nism is similar to that of the 65–80 wt % 3EG-water mixtures. The high-frequency secondary process is a Johari-Goldstein (β_{JG}) process of the 3EG molecules based on a coupling model proposed by Ngai and coworkers [23–28]. The characteristics of the secondary processes are different between the 65–80 wt % and 90–100 wt % 3EG-water mixtures. However, the relationship between the molecular dynamics above T_C and molecular mechanism of the α-β separation behavior for the 3EG-water mixtures is not clear yet.

The *a* process of the aqueous solutions above T_C reflects the molecular interaction based on the molecular structure of solute and water content. When the temperature decreases, the *a* process separates into the α and β processes below T_C. Thus, the molecular mechanism of the α-β separation behavior relates to the microscopic molecular environments above T_C, and the α-β separation behavior offers important bindings to understand the relaxation phenomena in the supercooled and glassy state of the aqueous solutions. In this work, the separation behavior for the 3EG-water mixtures as an example of the large solute-water mixtures is investigated, and the relationships between the molecular dynamics above T_C and the α-β separation behavior is discussed.

II. EXPERIMENT

The 3EG used in this experiment was purchased from Aldrich. Distilled and deionized water with an electric conductivity lower than 18.3 μS/m was obtained from ultrapure water products (Millipore, MILLI-Q Lab). Aqueous solutions of 65, 70, 80, 90, 94, and 100 wt % 3EG were prepared.

We used four dielectric measurement systems in order to cover the frequency range of 1 μHz–10 GHz. From 1 MHz to 10 GHz, time domain reflectometry (TDR) measurements were performed [29,30]. An LCR meter (HP 4284A) was used from 20 Hz to 1 MHz. We used an improved ac phase analysis (ACPA) method for the frequency range of 10 μHz–1 kHz [31]. For the range of 1 μHz–10 mHz, a dc transient current (DCTC) method was also improved using a subfemtoamp remote source meter (KEITHLEY 6430) [31]. The sample cell used for the TDR measurement in the frequency range of 1 MHz–1 GHz was a coaxial cylindrical electrode (air capacitance was 100 fF). For the TDR measurement in the frequency range higher than 1 GHz, the sample was placed at the end of the coaxial line (the diameters of center and outer conductors were 0.5 and 2.2 mm, respectively), and the end of the coaxial line acted as the electrode (the air capacitance was 10.0 fF). For TDR measurement, the temperature was controlled within an accuracy of ± 0.05 °C using a water bath. The sample cell used for the LCR meter, ACPA, and DCTC measurements in the frequency range below 1 MHz was a three-terminal coaxial cylindrical electrode (the air capacitance was 18.00 pF). The temperature of the sample cell was controlled at an accuracy of ± 0.1 °C using a cryostat (IWATANI GAS, CRT-006-6000).

III. RESULTS

Figure 1 shows the dielectric loss spectra for the 65 wt % and 80 wt % 3EG-water mixtures, and pure 3EG at various temperatures. For each mixture, a single loss peak is observed in the high-temperature range, and two loss peaks are clearly observed in the low-temperature range.

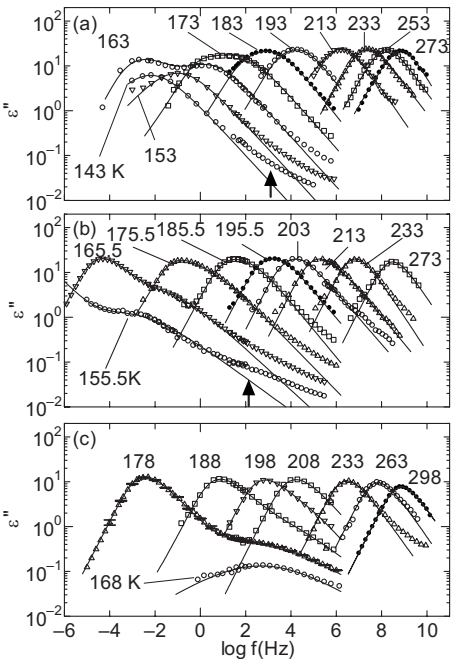

FIG. 1. Dielectric loss spectra for (a) 65 and (b) 80 wt % triethylenelglycol-water mixtures, and (c) pure triethyleneglycol at various temperatures. The solid line indicates the simple summation of the KWW and two Cole-Cole equations. The arrows indicate the deviation of the relaxation curve calculated from the experimental results.

Figure 2 shows the dielectric loss spectra for the 65, 80, and 100 wt % 3EG-water mixtures at 233.2 K in order to show the shape of the primary process called the *a* process [1] in the temperature range at which only one loss peak is observed. The loss spectra for the 80–100 wt % 3EG-water mixtures agrees well with the relaxation curve calculated using the KWW equation within the frequency range of ± 1.5

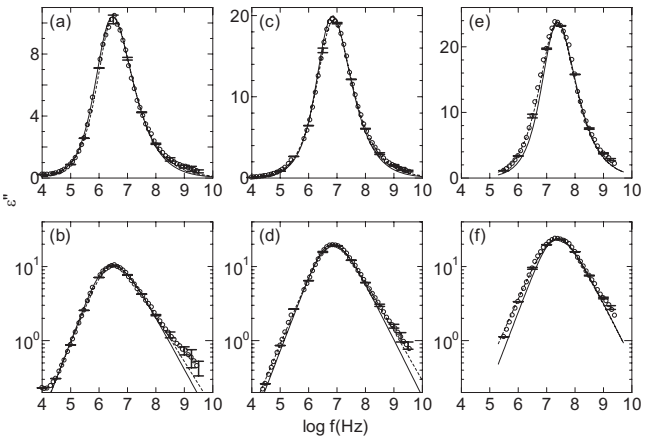

FIG. 2. Dielectric loss spectra for (a) and (b) 100, (c) and (d) 80, and (e) and (f) 65 wt % triethyleneglycol-water mixtures at 233 K. The solid and dotted lines indicate the results calculated using the KWW and HN equations, respectively.

decades around the loss peak frequency. The KWW equation is given by [8,9]

$$\varepsilon^*(\omega) = \varepsilon_\infty + (\varepsilon_S - \varepsilon_\infty)\int_0^\infty \left[-\frac{d\Phi(t)}{dt}\right]\exp(-j\omega t)dt. \quad (1)$$

Here,

$$\Phi(t) = \exp\left[-\left(\frac{t}{\tau}\right)^{\beta KWW}\right], \quad (2)$$

where t is the time, j is the imaginary unit, ε_S is the limiting low-frequency permittivity, ε_∞ is the limiting high-frequency permittivity, τ is the relaxation time, ω is the angular frequency, and β_{KWW} $(0<\beta_{KWW}\leqslant 1)$ quantifies the asymmetric broadening of a loss spectrum. Equation (2) with $\beta_{KWW}=1$ corresponds to the Debye-type relaxation. The β_{KWW} value of the 80–100 wt % 3EG-water mixtures is not unity. These results indicate that the loss spectrum for the 80–100 wt % 3EG-water mixtures shows a KWW-type asymmetric shape.

On the other hand, the dielectric loss spectra of the 65 and 70 wt % 3EG-water mixtures cannot be described by the KWW equation, showing a systematic deviation as shown in Figs. 2(e) and 2(f). This can be described well by the Havriliak-Negami (HN) equation within the frequency range of ±1.5 decades around the loss peak frequency. The HN equation is given by

$$\varepsilon^*(\omega) = \varepsilon_\infty + \frac{\varepsilon_S - \varepsilon_\infty}{[1+(j\omega\tau)^{\beta_{HN}}]^{\alpha_{HN}}}, \quad (3)$$

where $\alpha_{HN}(0<\alpha_{HN}\leqslant 1)$ and $\beta_{HN}(0<\beta_{HN}\leqslant 1)$ quantify the asymmetric and symmetric broadenings of a loss spectrum, respectively. Equation (3) with $\alpha_{HN}=1$ and that with $\beta_{HN}=1$ correspond to the Cole-Cole-type and Devidson-Cole-type relaxations, respectively. The shape parameters of the loss spectrum obtained by curve fitting for the 65 wt % 3EG-water mixture are $\alpha_{HN}=0.82$ and $\beta_{HN}=0.88$ (then $\alpha_{HN}\beta_{HN}=0.72$). The dielectric spectra for the pure 3EG and 80 wt % 3EG-water mixture can also be described well by the HN equation. The shape parameters obtained by curve fitting are $\alpha_{HN}=0.73$ and $\beta_{HN}=0.92$ $(\alpha_{HN}\beta_{HN}=0.67)$ for the 80 wt % 3EG-water mixture, and $\alpha_{HN}=0.65$ and $\beta_{HN}=0.94$ $(\alpha_{HN}\beta_{HN}=0.61)$ for the pure 3EG. These results indicate that α_{HN} increases and $\alpha_{HN}\beta_{HN}$ approaches the β_{HN} with increasing water concentration. The limiting behaviors of the loss spectra at the low- and high-frequency wings are characterized as [32]

$$\frac{\partial \log \varepsilon''(\omega)}{\partial \log \omega} = \beta_{HN} \quad (\omega \ll \tau^{-1}) \quad (4)$$

and

$$\frac{\partial \log \varepsilon''(\omega)}{\partial \log \omega} = -\alpha_{HN}\beta_{HN} \quad (\omega \gg \tau^{-1}), \quad (5)$$

respectively. When $\alpha_{HN}\beta_{HN}$ agrees with β_{HN}, the loss spectra show a Cole-Cole-type symmetric shape. The values of the shape parameters indicate that the loss spectra of the 65–70 wt % 3EG-water mixtures are more symmetric than those of the 80–100 wt % 3EG-water mixtures.

In the low-temperature range, the primary α process and the β_{JG} process are observed for the 90–100 wt % 3EG-water mixtures as shown in Fig. 1(c). The α process and β process, whose strength is much larger than that of the β_{JG} process, are observed for the 65–80 wt % 3EG-water mixtures. The dielectric spectra for the 65–100 wt % 3EG-water mixtures can be described by the simple summation of the KWW and Cole-Cole equations, and in terms of the dc conductivity,

$$\varepsilon^*(\omega) = \varepsilon\infty + \Delta\varepsilon_\alpha\int_0^\infty \left[-\frac{d\Phi(t)}{dt}\right]\exp(-j\omega t)dt + \frac{\Delta\varepsilon_\beta}{1+(j\omega\tau_\beta)^{\beta_{CC}}} + \frac{\sigma}{j\omega\varepsilon_0}, \quad (6)$$

and

$$\Phi(t) = \exp\left[-\left(\frac{t}{\tau_\alpha}\right)^{\beta KWW}\right].$$

Here, $\Delta\varepsilon$ is the relaxation strength and β_{CC} $(0<\beta_{CC}\leqslant 1)$ quantifies the symmetric broadening of a loss spectrum. σ is the dc conductivity, and ε_0 is the permittivity of free space. The subscripts α and β indicate the primary α process and secondary β or β_{JG} processes, respectively. In the frequency range +2 decades higher than the β process for 65 and 80 wt % 3EG-water mixtures, the deviation of the relaxation curve calculated from Eq. (6) from the experimental results is observed as indicated arrows in Figs. 1(a) and 1(b). This deviation is a contribution of an *excess-wing* or a high-frequency flank discussed tail of another relaxation process [33–36]. This work does not focus on the high-frequency process.

Figure 3 shows plots of relaxation time for the 65 and 80 wt % 3EG-water mixtures and pure 3EG against reciprocal temperature. The relaxation time of the a process, τ_a, for the 80–100 wt % 3EG-water mixtures continues to τ_α below the crossover temperature, T_C. On the other hand, τ_a for the 65–70 wt % 3EG-water mixtures seems to continue to τ_β below T_C. Here, the T_C of the pure 3EG is defined as the temperature at which the extrapolation from $\tau_{\beta JG}$ below T_g agrees with τ_α. The T_C of the 65–80 wt % 3EG-water mixtures cannot be defined from the Arrhenius diagram, because τ_β does not merge with τ_α. Thus, T_C is defined from the relaxation strengths of the 65–80 wt % 3EG-water mixtures as follows. The $\Delta\varepsilon_\beta$ for the 80 wt % 3EG-water mixture and $\Delta\varepsilon_\alpha$ for the 65 wt % 3EG-water mixture decrease with increasing temperature and become zero, as shown in Fig. 4. The T_C of the 65 wt % 3EG-water mixture is defined as the temperature at which $\Delta\varepsilon_\alpha$ becomes zero, and that of the 80 wt % 3EG-water mixture is defined as the temperature at which $\Delta\varepsilon_\beta$ becomes zero. The temperature dependence of τ_α for each mixture is described by the Vogel-Fulcher (VF) equation

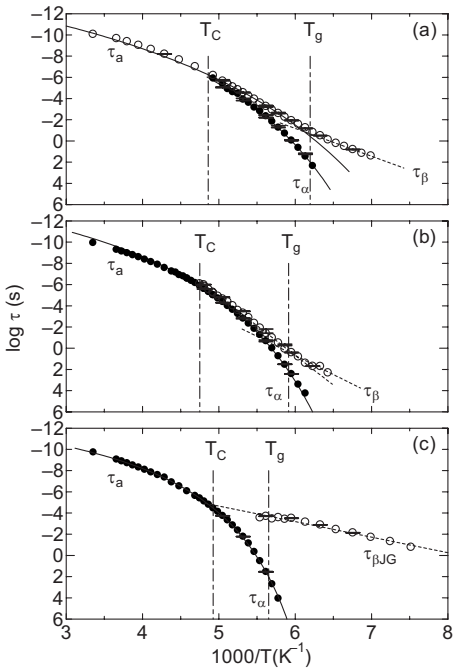

FIG. 3. Plots of the logarithm of relaxation time against reciprocal temperature for (a) 65, (b) 80, and (c) 100 wt % triethyleneglycol-water mixtures. The solid and dotted lines indicate the results calculated using the Vogel-Fulcher and Arrhenius equations.

$$\log \tau_\alpha = \log \tau_{\infty VF} + \frac{A}{T - T_0}, \tag{7}$$

where T is the temperature, and $\tau_{\infty VF}$, A, and T_0 are empirical VF parameters. The temperature dependence of $\tau_{\beta JG}$ for 90–100 wt % 3EG-water mixtures and τ_β for the

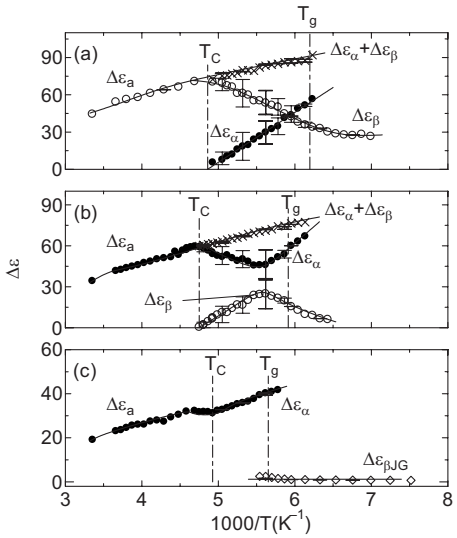

FIG. 4. Plots of relaxation strength against reciprocal temperature for (a) 65, (b) 80, and (c) 100 wt % triethyleneglycol-water mixtures. Crosses indicate the sums of the relaxation strengths of the α and β processes.

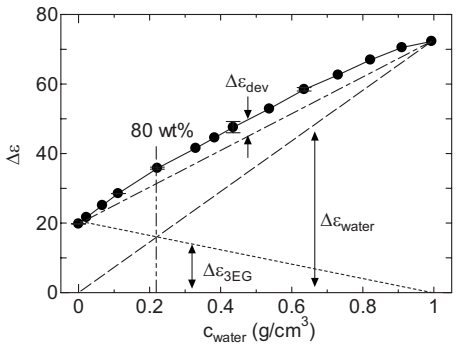

FIG. 5. Plots of water content against relaxation strength at 298 K. The dashed line connects the relaxation strength of 73.2 for pure water at c_{water}=0.994 and that of 0 at c_{water}=0. The dotted line connects the relaxation strength of 19.8 for pure 3EG at c_{water}=0 and 0 at that of c_{water}=0.994. The dashed-dotted line connects the relaxation strength of 73.2 for pure water and that of 19.8 for pure 3EG.

65–80 wt % 3EG-water mixtures below T_g is described by the Arrhenius equation

$$\log \tau_\beta = \log \tau_{\infty Arr} + \frac{\Delta E}{RT}, \tag{8}$$

where $\tau_{\infty Arr}$ is the pre-exponential factor, R is the gas constant, and ΔE is the apparent molar activation energy.

Figures 4(a)–4(c) show plots of relaxation strength for the 65, 80, and 100 wt % 3EG-water mixtures against reciprocal temperature. For the pure 3EG below T_C, the $\Delta\varepsilon_\alpha$ increases and $\Delta\varepsilon_{\beta JG}$ slightly decreases with decreasing temperature. For the 80 wt % 3EG-water mixture immediately below T_C, $\Delta\varepsilon_\alpha$ decreases when $\Delta\varepsilon_\beta$ increases with decreasing temperature, and it increases when $\Delta\varepsilon_\beta$ decreases with decreasing temperature. For the 65 wt % 3EG-water mixture, $\Delta\varepsilon_\alpha$ is observed at T_C, and it monotonically increases with decreasing temperature, and then $\Delta\varepsilon_\beta$ decreases. Cross symbols in Figs. 4(a) and 4(b) indicate the summation of $\Delta\varepsilon_\alpha$ and $\Delta\varepsilon_\beta$. The values of these parameters agree with the extrapolated values of the relaxation strength for the a process, $\Delta\varepsilon_a$, above T_C.

IV. DISCUSSION

For the results of the 80–100 wt % (low-water-content) 3EG-water mixtures, the a process above T_C continues to the α process below T_C, and additional secondary process is observed below T_C. On the other hand, for the 65–70 wt % (high-water-content) 3EG-water mixtures, the a process above T_C continues to the β process below T_C, and an additional α process is observed below T_C. These results indicate that the separation behavior clearly depends on the water content. First, we discuss the contribution of water to the a process for the 3EG-water mixtures on the basis of the water content dependences of the relaxation strength.

Figure 5 shows plots of relaxation strength for the 3EG-water mixtures against the water content, c_{water} (g/cm^3), at 25 °C, as an example that explains physical insights into the

a process, in order to estimate the contributions of water and 3EG molecules to the relaxation strength of the *a* process. The relaxation strength increases with increasing c_{water}, and this increase is not linear. The straight dashed line connects the relaxation strength of 73.2 for pure water at $c_{water}=0.994$ and that of 0 at $c_{water}=0$. The dotted line connects the relaxation strength of 19.8 for pure 3EG at $c_{water}=0$ and that of 0 at $c_{water}=0.994$. The dashed-dotted line connects the relaxation strength of 73.2 for pure water and that of 19.8 for pure 3EG. The dashed and dotted lines are assumed to indicate the contribution of water, $\Delta\varepsilon_{water}$, and that of 3EG, $\Delta\varepsilon_{3EG}$. The calculated $\Delta\varepsilon_{water}$ increases and $\Delta\varepsilon_{3EG}$ decreases with increasing c_{water} caused by an increase in the number of water molecules per unit volume. The ratio of $\Delta\varepsilon_{water}$ to $\Delta\varepsilon_{3EG}$ is unity at $c_{water}\cong 0.2$ (80 wt %), and $\Delta\varepsilon_{water}$ is larger than $\Delta\varepsilon_{3EG}$ in the high-water-content 3EG-water mixtures, $c_{water}>0.2$. The $\Delta\varepsilon_{water}+\Delta\varepsilon_{3EG}$ deviates from the relaxation strength observed, and this deviation, $\Delta\varepsilon_{dev}$, is small, $\Delta\varepsilon_{dev}/\Delta\varepsilon<10\%$. If $\Delta\varepsilon_{dev}$ is divided into the contribution of water and 3EG, the ratio of $\Delta\varepsilon_{water}$ to $\Delta\varepsilon_{3EG}$ is also unity at $c_{water}\cong 0.2$. These results suggest that the contribution of the water molecules to the *a* process is smaller than that of the 3EG molecules in the low-water-content (i.e., $c_{water}<0.2$) 3EG-water mixtures, and it becomes predominant in the high-water-content (i.e., $c_{water}>0.2$) 3EG-water mixtures.

It is noted that the *a* process for the low-water-content 3EG-water mixtures is the KWW-type asymmetric relaxation process. On the other hand, the *a* process for the high-water-content 3EG-water mixtures deviates from the KWW-type relaxation process, as shown in Fig. 2. The difference of the shape of loss spectrum can be discussed based on the contribution of water to the relaxation process. Generally, the α process for the various glass-forming materials shows the asymmetric shape of loss spectrum [1,2]. The primary loss spectrum of the water mixture of small associated liquids also shows the asymmetric shape [37,38]. These loss spectra are in good agreement with the relaxation curve calculated from the KWW equation. Convincing interpretations of the asymmetric loss spectrum for these kinds of materials are based on the cooperative motion of moving units. On the other hand, the symmetric loss spectrum has been observed for the relaxation process of water in the synthetic polymers- and biopolymers-water mixtures [20,37–43] and for the relaxation process of molecular liquids confined in porous systems [44,45]. The common feature of the molecules contributing to the relaxation process in these systems is that they are spatially confined and exist under a geometrical constraint. For the experimental results of the dielectric relaxation process of polymer-water mixtures, the relaxation time and the symmetric broadening of the relaxation process of water increases with increasing polymer concentration, and it can be explained by the geometrical self-similarity of the polymer network [40]. Therefore, the spatially restricted motion of water molecules under the geometrical constraint causes the symmetric broadening of the loss spectrum. For the results of the high-water-content 3EG-water mixtures [37], the water molecules can move cooperatively with around water molecules by hydrogen bonds. However, the 3EG molecules are too large to move cooperatively with water molecules, and then, the large 3EG molecule behaves as a geometrical constraint to the motion of water molecules. Therefore, the *a* process with deviation from the KWW-type relaxation process is caused by the contribution of uncooperative water molecules with the 3EG, predominantly. For the low-water-content 3EG-water mixtures, the water molecules also cannot move cooperatively with the 3EG molecules, but the contribution of the water molecules to the *a* process is much smaller than that of the 3EG. Then, the contribution of 3EG to the *a* process is predominant, and the cooperative motion of 3EG molecules leads to the KWW-type asymmetric loss spectrum. Therefore, the *a* process for the high-water-content 3EG-water mixtures is more symmetric than those of the low-water-content 3EG-water mixtures caused by the contribution of water to the *a* process, predominantly.

Next, the relationships between the molecular mechanism of the *a* process and the α-β separation behavior of the 3EG-water mixtures is discussed based on the contribution of water to the relaxation processes above and below T_C. We previously reported the water content dependence of the relaxation strengths for the 3EG-water mixtures below T_C [18]. For the low-water-content 3EG-water mixtures, $\Delta\varepsilon_\alpha$ increases with increasing c_{water} and reaches maximum at $c_{water}\cong 0.2$ (=80 wt %), and $\Delta\varepsilon_{\beta JG}$ is maintained constant. For the high-water-content 3EG-water mixtures, $\Delta\varepsilon_\beta$ increases with increasing c_{water}, and then $\Delta\varepsilon_\alpha$ decreases. These results can also be interpreted based on the cooperative motion of the water molecules with the 3EG molecules. For the low-water-content 3EG-water mixtures, the water molecules become able to move cooperatively with surrounding 3EG molecules below T_C, and this cooperative motion leads to the α process. It is noted that the local motions of 3EG lead to the β_{JG} process, because the β_{JG} process is observed at pure 3EG. For the high-water content 3EG-water mixtures, the number of water molecules, which cannot move cooperatively with the 3EG molecules, increases with decreasing 3EG molecules. Such uncooperative water molecules with 3EG molecules behave as "*excess water molecules*." The cooperative motion of water and 3EG molecules leads to the α process, and the motion of these excess water molecules leads to the β process. There results suggest that the molecular mechanism of the α and β processes is different between the low- and high-water-content 3EG-water mixtures. According to these results, the molecular mechanism of the α-β separation behaviors is discussed.

In particular, it is well known that the temperature dependence of the α process for most glasses shows the VF curve. According to Adam and Gibbs's theory, the VF curvature for the α process is related to the increase of size of the cooperative region, in which the reorientation of moving units occurred cooperatively, with decreasing temperature [11]. For the results of the Arrhenius diagram for the low-water-content 3EG-water mixtures in Fig. 3, the plotted curve from the *a* process at high temperature to the α process down to T_g is the VF type. Below T_C, some water molecules begin to move cooperatively with 3EG molecules and the cooperative motion of the water and 3EG molecules leads to the α process. On the other hand, for the high-water-content 3EG-water mixtures, the plotted curve from the *a* process at high temperature to the β process down to T_g is the VF type. This

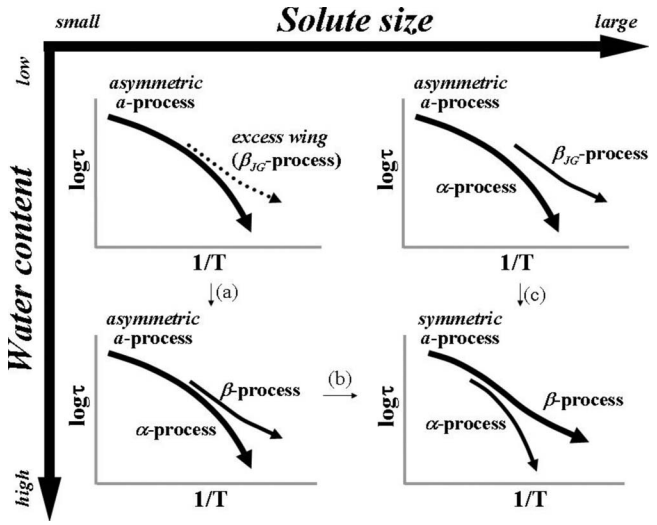

FIG. 6. Schematic representations of the α-β separation behavior for the small solute-water mixtures (left-hand side) large solute-water mixtures (right-hand side). (a) The results of the ethyleneglycol- and glycerol-water mixtures with various water content [13–15]. (b) The results of the 65 wt % ethyleneglycol oligomer-water mixtures [14,16]. (c) The results of the triethyleneglycol-water mixtures with various water content (this work).

result indicates that the size cooperative region of water increases with decreasing temperature. Below T_C, some water molecules also begin to move cooperatively with 3EG molecules and the cooperative motion of the water and 3EG molecules leads to the additional low-frequency α process. However, the excess water molecules are confined from the 3EG molecules and still contribute to the β process down to T_g. Therefore, the a process continuing to the β process is a result of the keep to contribute the water molecules.

It is already noted that the 3EG-water mixtures can be considered as an example of the large solute-water mixtures. Thus, the α-β separation behavior of the 3EG-water mixtures is compared with that of the small solute-water mixtures. Figure 6 shows schematically the α-β separation behavior depending on the molecular size and water content for alcohol-water mixtures reported [13–18]. The right-hand side of Fig. 6 corresponds to water mixtures with large solute molecules (large EGO- and polyethleneglyocol-water mixtures). In the low-water-content mixtures, the a process caused by the cooperative motion of solute molecules mainly is observed above T_C. This a process above T_C continues to the α process below T_C and additional β_{JG} processes are observed below T_C. It is also observed for many glass-forming polymers, such as polycarbonate, polyvinyl chloride, polychloroprene, and poly(ethylene terephthalate), and each polymer has a main dipole moment rigidly attached to the main chain. It is generally accepted that the cooperative motion of moving units in a main chain leads to the α process [1,2]. The β_{JG} process is brought about by the local motion of the main chain, and the relaxation strength of the β_{JG} process is much smaller than that of the α process in the whole temperature range observed [1,2]. For the high-water-content mixtures, the a process caused by the restricted motion of water from the polymer molecules mainly is observed above T_C. The a process above T_C continues to the β process below T_C, and the additional low-frequency α processes are observed below T_C. The temperature dependence of the relaxation parameters of the high-water-content large-solute mixtures is similar to that for Poly(n-alkyl-methacrylate)s and polyepoxy compounds [1,2,46]. The characteristic α-β separation behavior for the high-water-content large-solute mixtures is brought about by the following facts: (i) the a process is dominated by the main dipoles with high mobility, i.e., the water molecules. (ii) The water molecules begin to move cooperatively with the solute molecules below T_C. The uncooperative motion of the water with the solute molecules leads to the more symmetric shape of the a process. Immediately below T_C, the large β process continuing to the a process is caused by the contribution of many water molecules, and the cooperative motion of some water and 3EG molecules leads to the α process.

On the other hand, the left-hand side of the Fig. 6 corresponds to water mixtures with small solute molecules, such as ethyeleglycol and glycerol [13–16]. In the case of the low-water-content mixtures, the a process is observed in the whole temperature range measured, and the loss spectrum of the a process is the KWW-type asymmetric shape. Some decades above the loss peak frequency, an excess wing (also called "high-frequency wing" or "tail") shows up as a high-frequency excess contribution to the power law [33–36]. Recently, the excess wing has been discussed as the tail of the β_{JG} process [26]. For the high-water content mixtures, the KWW-type asymmetric a process caused by the cooperative motion of alcohol and water molecules is also observed above T_C. The KWW-type asymmetric a process above T_C continues to the α process below T_C, and the additional β process with large relaxation strength are observed below T_C. For the high-water-content small-solute mixtures, the cooperative motion of some alcohol and solute molecules mainly contributes to the a process. The uncooperative water molecules with the solute are also coexistent, and these water molecules behave as the excess water molecules. Below T_C, the contribution of the excess water molecules separated from the α process is observed as the β process.

It is concluded that the molecular mechanism of the α and β processes for the high-water content large-solute mixtures is similar to that for the high-water-content small-solute mixtures. However, the separation behaviors for these water-mixtures are different caused by the difference in the molecular mechanism of the a process.

V. CONCLUSION

We performed broadband dielectric measurements for 3EG-water mixtures with various water contents in the frequency range of 1 μHz–10 GHz and in the temperature range of 130–298 K. In the water concentration range at which the contribution of the 3EG molecules to the a process is predominant, the a process continues to the α process below T_C, and the additional β process is observed at the frequencies higher than that of the α process below T_C. On the other hand, in the water concentration range at which the

contribution of the water molecules to the a process is predominant, the a process continues to the β process below T_C, and the additional α process is observed at the frequencies lower than that of the β process below T_C. In this water concentration range, some water molecules begin to move cooperatively with the 3EG molecules below T_C, and this cooperative motion leads to the α process. The motion of the excess water molecules, which cannot move cooperatively with 3EG, leads to the β process. The difference in the α-β separation scenario in the low-temperature range between the high- and low-water-content 3EG-water mixtures is brought about by the dominance of the water and 3EG molecules above T_C.

ACKNOWLEDGMENTS

This work was supported by the Ministry of Education, Culture, Sports, Science, and Technology, Grant-in-Aid for Scientific Research on Priority Areas "Water and Biomolecules" (No. 18031034) and the Sasakawa Scientific Research Grant from the Japan Science Society.

[1] E. Donth, *The Glass Transition* (Springer, N.Y., 2001).
[2] A. Schönhals, in *Dielectric Spectroscopy of Polymeric Materials*, edited by J. P. Runt and J. J. Fitzgerald (American Chemical Society, Washington, D.C., 1997), Chap. 3.
[3] C. T. Moynihan, P. B. Macedo, C. J. Montrose, P. K. Gupta, M. A. DeBolt, J. F. Dill, B. E. Dom, P. W. Drake, A. J. Easteal, P. B. Elterman, R. P. Moeller, H. Sasabe, and J. A. Wilder, Ann. N.Y. Acad. Sci. **279**, 15 (1976).
[4] B. Schiener and R. Böhmer, J. Non-Cryst. Solids **182**, 180 (1995).
[5] C. León, K. L. Ngai, and C. M. Roland, J. Chem. Phys. **110**, 11585 (1999).
[6] H. Vogel, Phys. Z. **22**, 645 (1921).
[7] G. S. Fulcher, J. Am. Ceram. Soc. **8**, 339 (1923).
[8] R. Kohlrausch, Ann. Phys. **167**, 179 (1854).
[9] G. Williams and D. C. Watts, Trans. Faraday Soc. **66**, 80 (1971).
[10] D. W. Davidson and R. H. Cole, J. Chem. Phys. **18**, 1417 (1950).
[11] G. Adam and J. H. Gibbs, J. Chem. Phys. **43**, 139 (1965).
[12] P. O. Maurin, J. Chem. Phys. **109**, 10936 (1998).
[13] S. Sudo, N. Shinyashiki, and S. Yagihara, J. Mol. Liq. **90**, 113 (2001).
[14] S. Sudo, M. Shimomura, T. Saito, T. Kashiwagi, N. Shinyashiki, and S. Yagihara, J. Non-Cryst. Solids **305**, 197 (2002).
[15] S. Sudo, M. Shimomura, N. Shinyashiki, and S. Yagihara, J. Non-Cryst. Solids **307-310**, 356 (2002).
[16] S. Sudo, M. Shimomura, S. Tsubotani, N. Shinyashiki, and S. Yagihara, J. Chem. Phys. **121**, 7332 (2004).
[17] S. Sudo, M. Shimomura, K. Kanari, N. Shinyashiki, and S. Yagihara, J. Chem. Phys. **124**, 044901 (2006).
[18] N. Shinyashiki, S. Sudo, S. Yagihara, A. Spanoudaki, A. Kyritsis, and P. Pissis, J. Phys.: Condens. Matter **19**, 205113 (2007).
[19] K. Grzybowska, A. Grzybowski, S. Pawlus, S. Hensel-Bielowka, and M. Paluch, J. Chem. Phys. **123**, 204506 (2005).
[20] S. Cerveny, G. A. Schwartz, Á. Alegría, R. Bergman, and J. Swenson, J. Chem. Phys. **124**, 194501 (2006).
[21] S. Cerveny, Á. Alegría, and J. Colmenero, Phys. Rev. E **77**, 031803 (2008).
[22] S. Cerveny, Á. Alegría, and J. Colmenero, J. Chem. Phys. **128**, 044901 (2008).
[23] S. Capaccioli, K. L. Ngai, and N. Shinyashiki, J. Phys. Chem. B **111**, 8197 (2007).
[24] K. L. Ngai, Phys. Rev. E **57**, 7346 (1998).
[25] K. L. Ngai, J. Chem. Phys. **109**, 6982 (1998).
[26] M. Paluch, S. Pawlus, S. Hensel-Bielowka, E. Kaminska, D. Prevosto, S. Capaccioli, P. A. Rolla, and K. L. Ngai, J. Chem. Phys. **122**, 234506 (2005).
[27] K. L. Ngai, Comments Solid State Phys. **9**, 121 (1979).
[28] K. L. Ngai, R. W. Rendell, A. K. Rajagopal, and S. Teitler, Ann. N.Y. Acad. Sci. **484**, 150 (1986).
[29] R. H. Cole, S. Mashimo, and P. J. Winsor IV, J. Phys. Chem. **786**, 87 (1984).
[30] S. Mashimo, T. Umehara, T. Ota, S. Kuwabara, N. Shinyashiki, and S. Yagihara, J. Mol. Liq. **36**, 135 (1987).
[31] R. Nozaki and S. Mashimo, J. Chem. Phys. **87**, 2271 (1987).
[32] F. Kremer and A. Schönhals, *Broadband Dielectric Spectroscopy* (Springer, New York, 2002).
[33] U. Schneider, P. Lunkenheimer, R. Brand, and A. Loidl, Phys. Rev. E **59**, 6924 (1999).
[34] R. Brand, P. Lunkenheimer, U. Schneider, and A. Loidl, Phys. Rev. Lett. **82**, 1951 (1999).
[35] R. Brand, P. Lunkenheimer, and A. Loidl, Phys. Rev. B **56**, R5713 (1997).
[36] U. Schneider, R. Brand, P. Lunkenheimer, and A. Loidl, Phys. Rev. Lett. **84**, 5560 (2000).
[37] N. Shinyashiki, S. Sudo, W. Abe, and S. Yagihara, J. Chem. Phys. **109**, 9843 (1998).
[38] S. Sudo, N. Shinyashiki, Y. Kitsuki, and S. Yagihara, J. Phys. Chem. A **106**, 458 (2002).
[39] N. Shinyashiki, S. Yagihara, I. Arita, and S. Mashimo, J. Phys. Chem. B **102**, 3249 (1998).
[40] N. Shinyashiki and S. Yagihara, J. Phys. Chem. B **103**, 4481 (1998).
[41] Y. E. Ryabov, Y. Feldman, N. Shinyashiki, and S. Yagihara, J. Chem. Phys. **116**, 8610 (2002).
[42] Y. Hayashi, N. Shinyashiki, and S. Yagihara, J. Non-Cryst. Solids **305**, 328 (2002).
[43] Y. Hayashi, I. Oshige, Y. Katsumoto, S. Omori, and A. Yasuda, J. Non-Cryst. Solids **353**, 4492 (2007).
[44] J. Schüller, Yu. B. Mel'nichenko, R. Richert, and E. W. Fischer, Phys. Rev. Lett. **73**, 2224 (1994).
[45] J. Schüller, R. Richert, and E. W. Fischer, Phys. Rev. B **52**, 15232 (1995).
[46] S. Corezzi, E. Campani, P. A. Rolla, S. Capaccioli, and D. Fioretto, J. Chem. Phys. **111**, 9343 (1999).